CrystEngComm

Accepted Manuscript

ROYAL SOCIETY OF CHEMISTRY

www.rsc.org/crystengcomm

CrystEngComm

ARTICLE

Structure modulation, band structure, density of states and luminescent properties of columbite-type $ZnNb_2O_6$

Dan Zhao,[*a] Fa-Xue Ma,[a] Rui-Juan Zhang,[a] Fei-Fei Li,[a] Lei Zhang,[a] Juan Yang,[a] Yun-Chang Fan,[a] Xia Xin[b]

Received 00th January 20xx,
Accepted 00th January 20xx

DOI: 10.1039/x0xx00000x

www.rsc.org/

Zinc niobate $ZnNb_2O_6$， with columbite-type structure， has long been known as a promising dielectric, photocatalytic and luminescent material, yet the crystal structure has not been studied in full detail. For the first time, we re-determined the crystal structure using the single crystal X-ray diffraction method and established the commensurately modulated structure model through high-dimensional formalism. The structure features a (3+1)-dimensional superspace group *Pbcn*(α00)00*s* with the modulation vector q = 1/3*a. At the same time, the calculations of band structure and density of states were performed using the density functional theory to reveal the electronic origins of optical transitions. In addition, the photoluminescent properties of $ZnNb_2O_6$ were studied, revealing that a broad emission band at approximately 470 nm can achieve a high quantum efficiency up to 64% with an optimal sintered temperature of 950 °C.**

Introduction

Zinc niobate $ZnNb_2O_6$ is a promising semiconductor material for its interesting physical properties and potential applications as dielectric material, [1,2] photocatalysts [3, 4] and luminescent material.[5] Its chemical and thermal stability and the fact that it is relatively simple to prepare ensures the possibility for wide application in many fields. Generally speaking, it is the most foundational work to know the detailed crystal structure of a solid state material for further studying its physical properties. For $ZnNb_2O_6$, the crystal structure was reported to be a columbite-type structure with the orthorhombic space group *Pbcn* and cell parameters *a* = 14.21 Å, *b* = 5.73 Å, and *c* = 5.04 Å. [6, 7] Alternatively, this structure can be considered as a cationic ordered α-PbO_2

[a] *Department of Physics and Chemistry, Henan Polytechnic University, Jiaozuo 454000, China. E-mail: iamzd1996@163.com*
[b] *National Engineering Technology Research Center For Colloidal Materials, Shandong University, Jinan 250100, China.*

Electronic Supplementary Information (ESI) available: EDS analysis of $ZnNb_2O_6$ (Fig. S1); CIF file of $ZnNb_2O_6$; CheckCIF file of $ZnNb_2O_6$. See DOI: 10.1039/x0xx00000x

structure,[8] in which Zn^{2+} and Nb^{5+} cations alternatively occupy half of the octahedral cavities that are constructed by an oxygen ionic lattice. The structure contains two-dimensional (2D) ZnO_6 layers and NbO_6 layers, which are stacked along the *a*-axis in the sequence of Zn—Nb—Nb—Zn—Nb—Nb to from a 3D framework. However, previous structural studies for compound $ZnNb_2O_6$ were confined to X-ray powder diffraction (XRD), and the results were not very crystallographically satisfied. Thus we made an effort to grow single crystals and determine the structure using the single-crystal X-ray diffraction method. The results show that compound $ZnNb_2O_6$ features an *a*-axis tripled super structure, or in other words, a (3+1)-dimensional commensurately modulated structure.

Modulated crystal, whose structure has no translational symmetry in the 3D space, can be considered as a periodic structure in a higher than 3D space. The lack of translational periodicity in one, two, or three dimensions of the physical space can be described by one, two, or three modulation waves in different directions. To restore the periodicity, it is necessary to transform the data into (3 + n)D (n = 1, 2 or 3) spaces. In such high-dimensional descriptions, atoms are no longer discrete objects, but 1D "atomic surfaces" and the reciprocal space vectors are generally expressed as H = ha^* + kb^* +lc^* + mq (a^*, b^*, and c^* are the basis vectors of the 3D reciprocal lattice). The modulation vector can be expressed as **q** = αa^* + βb^* + γc^*, where α, β, and γ are numbers that are rational for commensurate cases and irrational for incommensurate cases. In recent years, many new modulated crystals including organic, metal-organic and inorganic compounds have been perfectly modelled through the superspace formalism approach, including $LaSeTe_2$,[9] (2-methylimidazolium) tetraiodobismuthate(III),[10] $Ba_2Cu_2Te_4O_{11}Br_2$,[11] $Ho(PO_3)_3$,[12] $CaGd_{2(1-x)}Eu_{2x}(MoO_4)_{4(1-y)}(WO_4)_{4y}$ ($0\le x\le 1$, $0\le y\le 1$),[13] $[CaNd]_2[Ga]_2[Ga_2O_7]_2$,[14] $LiCuVO_4$,[15] $C_{10}H_{16}N_6S$,[16] $Ba_{1+x}[(Cu_xRh_{1-x})O_3]$ (x = 0.1605, 0.1695),[17] and $[N(CH_3)_4]_2MeCl_4$,[18]. The most famous sample is the series of perovskite-type high-Tc superconductors, whose structures are usually commensurately or incommensurately modulated, such as $YBa_2Cu_3O_{6+x}$ [19, 20] and $Bi_2Sr_{3-x}Ca_xCu_2O_{8+y}$.[21]

In this paper, we will present the synthesis, crystal structure determination through a high-dimensional crystallographic approach and a spectral measurement for compound $ZnNb_2O_6$. Moreover, we also calculate the crystal energy band structures and density of states (DOS) to understand the chemical bonding properties and electronic origin of optical transitions.

Experimental

Materials and instrumentation

All of the chemicals were analytically pure from commercial sources and used without further purification. KCl, K_2CO_3, ZnO and Nb_2O_5 were purchased from the Shanghai Reagent Factory (Shanghai, China). Microprobe elemental analysis was performed by a field-emission scanning electron microscope equipped with an energy-dispersive X-ray spectroscope (EDS, JSM6700F, Oxford INCA). X-Ray powder diffraction (XRD) patterns were collected on an RIGAKU DMAX2500 diffractometer using graphite-monochromated CuKα radiation in the angular range 2ϑ = 5—75° with a step size of 0.02°. The optical diffuse reflectance spectrum was measured with a spectrophotometer JASCO V550 equipped with an integrating sphere in the wavelength range of 200—850 nm at room temperature. The instrument was equipped with an integrating sphere, and $BaSO_4$ powder was used as a reference for baseline corrections. The absorption spectra were determined using the diffuse-reflectance technique. Photoluminescent properties were performed on an EDINBURGH FLS980 fluorescence spectrophotometer with an excitation wavelength of 520 nm. White $BaSO_4$ (reflection 100%) was used as the standard reference for reflection measurements.

Preparation

A single-crystal of $ZnNb_2O_6$ was initially prepared using the high-temperature solution growth (HTSG) method using K_2CO_3—KCl as the flux. The initial reagents of K_2CO_3 (0.500 g, 3.62 mmol), KCl (5.00 g, 67.1 mmol), ZnO (0.0814 g, 1 mmol) and Nb_2O_5 (0.266 g, 1 mmol) was thoroughly ground in an agate mortar and pressed into a pellet to ensure the best homogeneity and reactivity. Next, the mixture was put into a platinum crucible and was transferred into an oven and heated at 1000 °C in the air for 20 h. The mixture was completely melted at this stage, and then allowed to cool at a rate of 2 °C·h^{-1} to 700 °C before turning off the furnace. After being boiled in water, the prism-shaped colourless crystals were purified to a very low yield (<5%). The atomic ratio of $ZnNb_2O_6$ was determined using energy-dispersive spectrometry (EDS) for asingle crystal. The resultsagreed with what was determined from the structural analysis using single-crystal X-ray diffraction (see Supplementary information, Fig. S1).

After proper structural analysis, a pure powder sample compound $ZnNb_2O_6$ was obtained quantitatively from the solid state reaction of an Nb_2O_5/ZnO mixture in a molar ratio of 1 : 1. The mixture was thoroughly ground in an agate mortar and pressed into a pellet. Then, it was divided into seven parts and calcined in a platinum crucible for 48 h at 800 °C, 850 °C, 900 °C, 950 °C, 1000 °C, 1050 °C and 1150 °C with several intermediate grinding stages to ensure a complete solid state reaction. Through XRD powder diffraction studies it was proven that all seven samples were successfully obtained in a single phase (Fig. 1). It is worth mentioning that the samples used for spectral measurements are polycrystalline powders synthesized by solid-state reactions.

X-ray crystal determination

A suitable single crystal with dimensions of 0.20 × 0.05 × 0.05 mm was selected and mounted on a glass fibre for the single-crystal X-ray diffraction experiment. The intensity data were collected using a Bruker Smart Apex II CCD [22] single-crystal diffractometer system equipped with a graphite-monochromated *Mo-Kα* radiation source (λ = 0.71073 Å) over an angular range of 2.87°—28.27° with an exposure time of 10 s/deg. The frames were collected at ambient temperature with a scan width of 0.5° in ω and integrated with the *Saint*

software package using a narrow-frame integration algorithm. Diffraction patterns show strong main reflections and weak satellite reflections, clearly indicating a modulated structure. Then, using the Reciprocal lattice viewer (RLATT) tool, the reciprocal space was constructed from the experimental single crystal diffraction data, showing the main reflections, satellite reflections and modulation vectors along the *a**-axis. The main reflections could be indexed on the basis of an orthorhombic unit cell, and the satellite reflections besides the normal Bragg reflections could be indexed based on a commensurate modulation vector, **q** = 1/3*a**, where *a** is the reciprocal lattice vector. The scale module, deployed within Apex II, was used for multi-scan absorption corrections to generate *.p4p and *.hk6 files for the structure solution. After that, the crystal structure of $ZnNb_2O_6$ was determined by the charge-flipping method using the *Superflip* programme [23] and was subsequently refined by the *Jana2006* crystallographic computing system [24]. All of the atoms in the structure were refined using harmonic anisotropic atomic displacement parameters (ADP). The details of the data collection and structure refinement are summarized in Tab. 1, and further detailsabout the crystal structure investigations can be obtained from the Fachinformationszentrum Karlsruhe, 76344 Eggenstein-Leopoldshafen, Germany (fax: (49)7247-808-666; e-mail: crysdata@fizkarlsruhe.de), quoting the depository number CSD-430203.

Table 1. Experimental details for the data collection and structural refinement details of $ZnNb_2O_6$

Crystal data	
Chemical formula	$Nb_{2.667}O_8Zn_{1.333}$
M_r	462.9
Crystal system, space group	Orthorhombic, *Pbcn*(α00)00*s*
Temperature (K)	293(2)
Modulation wave vector	**q** = 1/3 *a**
a, *b*, *c* (Å)	4.7283 (4), 5.7208 (4), 5.0331 (5)
V (Å^3)	136.14 (2)
Z	1
Radiation type	Mo *K*α
μ (mm^{-1})	11.28
Crystal size (mm)	0.20 × 0.05 × 0.05
Diffractometer	Bruker APEX II CCD
Absorption correction	Multi-scan
range of *h*, *k*, *l* and *m*	$-6 \le h \le 6$ $-7 \le k \le 7$ $-6 \le l \le 6$ $-1 \le m \le 1$
No. of measured, independent and observed [$I > 3\sigma(I)$] reflections	3459, 513, 419
No. of observed main reflections and first order reflections	155, 264
R_{int}	0.027
$(\sin \vartheta/\lambda)_{max}$ (Å^{-1})	0.666
$R[F^2 > 2\sigma(F^2)]$, $\omega R(F^2)$, *S*	0.015, 0.015, 1.17
No. of reflections	513
No. of parameters	31
$\Delta\rho_{max}$, $\Delta\rho_{min}$ (*e*·Å^{-3})	0.43, −0.73

Computational description

The super structure model (3×*a*) of $ZnNb_2O_6$ determined by X-ray was used for the theoretical calculations. Band structure calculations along with density of states (DOS) were carried out with the density functional theory (DFT) using one of the non-local gradient-corrected exchange–correlation functions (GGA-PBE) and performed with the CASTEP code,[25-27] which uses a plane wave basis set for the valence electrons and core electrons.[28] The number of plane waves included in the basis was determined by a cut-off energy of 340.0 eV and the numerical integration of the Brillouin zone was performed using a 2×4×5 Monkhorst-Pack *k*-point sampling. The interactions between the ionic cores and the electrons were described by the ultrasoft pseudopotential, in which the orbital electrons of Zn-3$d^{10}4s^2$, Nb-4$s^2$4$p^6$4$d^4$5s^1 and O-2$s^2$2p^4 were treated as valence electrons.

Results and discussion

Crystal structure

For commensurately modulated cases, the structural solutions could usually be fulfilled using the superstructure method. However, our initial structural solution for $ZnNb_2O_6$ using the superstructure method with space group *Pbcn* (*a* = 14.1897(15), *b* = 5.7223(6), *c* = 5.0345(5)) yields non-positive

definite atomic displacement parameters for Zn and O atoms, large 'unexplainable' residual peaks, and a large *R* value greater than 0.09. A careful examination of the reciprocal lattice constructed from the experimental single crystal diffraction data of $ZnNb_2O_6$ (Fig. 2) showed that alternating the stronger and weaker spots along the *a**-axis is the characteristic of modulated structure. Hence, the more scientific and effective approach, superspace formalism was used to solve and refine the modulated structure of compound $ZnNb_2O_6$.

High-dimensional space groups were tested using the Jana2006 software, and it was determined that all of the observed reflections fulfilled the reflection conditions for the 4D superspace group *Pbcn*(*α*00)00*s*, a space group that belongs to the (3 + 1)D subset of the 4D space groups. In this nomenclature, the *Pbcn* component indicated that the (3 + 1)D symmetry operations were derived from this 3D space group, and the "(*α*00)" tells us that the **q** vector has one component of *a**. Within the 4D superspace formalism approach, an additional coordinate x_4 can be expressed as $x_4 = t + \mathbf{q}\cdot\mathbf{x}$, where $\mathbf{x} = (x_1, x_2, x_3)$ is the physical-space coordinate with respect to the lattice, and the t ($0 \le t \le 1$) parameter is the distance between a point and physical space.

The structural solution was performed using the Superflip programme assuming kinematic diffraction intensities and then generated 3 atomic positions including one O atom, one Zn atom and one Nb atom. The Zn and Nb atoms statistically occupy the same position (noted as Zn|Nb) as listed in Tab. 2. As shown in Fig. 3a, 3b and 3c, the O atom is only moderately modulated and can be explained by one displacive modulation function. However, Fourier syntheses revealed that the Zn|Nb atom showed a discontinuity, and a crenel function was chosen and successfully applied for the Zn|Nb atom with parameters $x_4^0 = 0$ (Zn) and $x_4^0 = 0.5$ (Nb) and an occupation parameter delta = 0.5 for both atoms (Fig. 3d, 3e and 3f). The final refined occupation parameters (Zn : Nb = 1 : 2) that achieved charge balance and satisfied the results of the EDX analysis were fixed for further calculations. In fact, the order of Zn and Nb atom can be considered as the primary parameter of the structure modulation. The structural model was successfully refined using isotropic atomic displacement parameters (ADPs), which gave acceptable values of $R = 0.015$ for main reflections and a slightly higher value of $R = 0.0294$ for first order satellites. Moreover, different Fourier syntheses using the final atomic parameters showed no significant residual peaks (highest residual peak of 0.43 $e\cdot Å^{-3}$ and highest residual hole of -0.73 $e\cdot Å^{-3}$). Therefore, we deemed that our commensurately modulated refined model for $ZnNb_2O_6$ was reasonable.

Table 2. Fractional atomic coordinates and isotropic or equivalent isotropic displacement parameters ($Å^2$) for $ZnNb_2O_6$

	x	*y*	*z*	U_{iso}*/U_{eq}	Occ. (<1)
Nb1	0	0.82060 (4)	0.25	0.00508 (8)	0.6667
Zn1	0	0.82060 (4)	0.25	0.00508 (8)	0.3333
O1	0.2284 (2)	1.1149 (2)	0.4190 (2)	0.0060 (3)	

The accuracy of our commensurately modulated structural model for $ZnNb_2O_6$ could be confirmed by powder diffraction analysis. Using the traditional high-temperature solid-state reaction method, a powder pattern of $ZnNb_2O_6$ can be obtained by powder X-ray diffraction analysis. As shown in Fig. 1, the simulated pattern fits very well with the experimental pattern in the 2ϑ range of 5–65°. Although satellite reflections are very weak in the powder diffraction pattern using Cu Kα as the X-ray source, some satellite peaks could still be seen in some regions, such as (1 0 0 -1) and (0 1 0 1) at approximately 15°. Hence, we concluded that our structural model is correct, and our powder pattern is pure.

The 3×*a** supercell model as an approximate representation of the atomic structure was shown in Fig. 4. Both Zn and Nb atoms are octahedrally coordinated by six O atoms into the ZnO_6 and NbO_6 octahedra, which were interconnected via edge-sharing O atoms to form Zn–O layers and Nb–O layers, respectively. Furthermore, the Zn–O and Nb–O layers are stacked along the *a*-axis to form the 3D framework of the compound $ZnNb_2O_6$. The bond distance of Nb–O, whose strong modulations were described by the crenel function in the 4D description, is 2.016 Å on average and is distributed between lengths of 1.803(2) Å and 2.270(2) Å. Similarly, the Zn–O bond distances is 2.105 Å on average and is distributed between lengths of 2.061(2) Å and 2.172(2) Å (Tab. 3). The detailed distributions of the Nb–O and Zn–O distances were drawn in Fig. 5. We can see that the NbO_6 octahedra tends to be distorted more than the ZnO_6 octahedra, which can be attributed the second-order Jahn–Teller (SOJT) effection of the d^0 electronic structure of the centred Nb^{5+} ion.

Table 3 Select interatomic distances in the modulated structure of $ZnNb_2O_6$

	Average	Minimum	Maximum
Nb1—O1	2.178(2)	2.085(2)	2.270(2)
Nb1—O1^{iii}	2.178(2)	2.085(2)	2.270(2)
Nb1—O1^{ii}	1.992(2)	1.920(2)	2.065(2)
Nb1—O1^{iv}	1.879(2)	1.803(2)	1.954(2)
Nb1—O1^{v}	1.992(2)	1.920(2)	2.065(2)
Nb1—O1^{vi}	1.879(2)	1.803(2)	1.954(2)
Zn1—O1	2.172(2)	2.172(2)	2.172(2)
Zn1—O1^{iii}	2.172(2)	2.172(2)	2.172(2)
Zn1—O1^{ii}	2.082(2)	2.082(2)	2.082(2)
Zn1—O1^{iv}	2.061(2)	2.061(2)	2.061(2)
Zn1—O1^{v}	2.082(2)	2.082(2)	2.082(2)
Zn1—O1^{vi}	2.061(2)	2.061(2)	2.061(2)
Symmetry codes: (i) $-x_1, -x_2+2, -x_3, -x_4$; (ii) $-x_1, -x_2+2, -x_3+1, -x_4$; (iii) $-x_1, x_2, -x_3+1/2, -x_4$; (iv) $x_1-1/2, x_2-1/2, -x_3+1/2, x_4+1/2$; (v) $x_1, -x_2+2, x_3-1/2, x_4$; (vi) $-x_1+1/2, x_2-1/2, x_3, -x_4+1/2$.			

In addition, it is useful to calculate the bond valence sums (BVS) to evaluate the validity of the commensurately modulated structural model. [28] The average values in the

modulated structure are 4.867, 2.046 and 1.929 for the Nb, Zn and O atoms, respectively, which are within the tolerable range.

Band structure, density of states and chemical bonds

The calculated band structure of $ZnNb_2O_6$ (3×*a** supercell model) along the high-symmetry points of the first Brillouin zone were plotted in Fig. 6. It was observed that both the top of the valence bands (VBs) and the bottom of the conduction bands (CBs) are very flat. The lowest energy of CBs and the highest energy (0.00 eV) of VBs are localized at different points between points G and Z, respectively. Therefore, compound $ZnNb_2O_6$ is a semiconductor with an indirect band-gap.

The experimental optical diffuse reflectance absorption spectrum of $ZnNb_2O_6$ was measured in the range of 200–850 nm. As shown in Fig. 7, little absorption was observed in the range of 350–850 nm, and the absorption edge is around 320 nm (3.87 eV) , which might be considered the band gap of $ZnNb_2O_6$. It should be noted that there is a weak absorption peak at about 350 nm, which may originate from crystalline defects because the traditional high-temperature solid state reaction can easily lead to such defects. Compared to the experimental band gap, the calculated band gap of 3.50 eV was small. This discrepancy was due to the limitations of the DFT method that generally underestimates the band gap of semiconductors and insulators. [30-32] Hence, a scissor operator of 0.37 eV was applied to perform calculations for the DOS analysis.

The density of total states (TDOS) of $ZnNb_2O_6$ and projected the density of states (PDOS) for the Zn, Nb and O elements ranging from -57 to 12 eV were calculated by PBE. as shown in Fig. 8. The regions below the Fermi level contain 178 bands and can be divided into five regions. The bottom-most VB region with an energy around -54.5 eV is composed of Nb-4*s* states, while the second region at around -31.0 eV is composed of Nb-4*p* states. The third region at around -16.5 eV is mainly composed of O-2*s* states mixed with a small amount of Nb-5*s* states. The forth region ranging from -2.0 eV to -6.0 eV arises mainly from a mixture of Zn-3*d*, Nb-4*d* and O-2*p* states. The highest VB region just below the Fermi level is dominated by the O-2*p* states, mixed with a small amount of the Zn-3*d* and Nb-4*d* states. On the other hand, the CBs just above the Fermi level are composed of a mixture of of Nb-4d and O-2p states. Therefore, we can say that the Zn/Nb atoms and O atoms are covalently joined together. Additionally, we also believed that the optical absorptions at the low energy region (about 320 nm) could be ascribed mainly to the charge transitions from the O-2*p* states to the Nb-4*d* states. In other words, the spectra absorption band can be attributed to a charge transfer from the oxygen ligands to the central Nb atom inside the NbO_6 groups.

In addition, we used the population analysis to elucidate the nature of the electronic band structure and chemical bonds. The calculated Mulliken bond orders of the Zn–O and Nb–O bonds are 0.12–0.27 and 0.24–0.82 e (covalent single-bond order is generally 1.0 e), respectively. Therefore, we can say that the covalent character of the Nb–O bond is larger than that of the Zn–O bond, and the ionic character of the Zn–O bond is larger than that of the Nb–O bond.

Photoluminescent properties

The self-activated photoluminescent properties of compound $ZnNb_2O_6$ were studied previously, revealing a very strong blue luminescence at room temperature.[33,34] In our work, we re-studied the self-activated photoluminescent properties of $ZnNb_2O_6$ sintered at a temperature ranging from 800 ºC to 1150 ºC..

As shown in Fig. 9a, the excitation data of $ZnNb_2O_6$ fired at 950°C by monitoring the main blue-violet fluorescence at a wavelength of 470 nm were recorded from 200 to 300 nm. Considering the above discussion of the density of states (Fig. 8), the broad band between 240 nm to 300 nm can be assigned to the O → Nb charge transfer (CT) transition. It should be noted that a sharp band at around 235 nm is only the second diffracted emission light by monitoring the fluorescence of 470 nm. Fig. 9b shows the emission spectra of the $ZnNb_2O_6$ sample excited at a wavelength of 278 nm. Because the conduction band is composed of Nb-4*d* orbitals and the valence band is composed of O-2*p* orbitals, we think that the strong blue-violet emission band centred at 470 nm can be attributed to the self-trapped exaction recombination of the NbO_6 groups. Moreover, with the increasing sintering temperature, the emission intensity of the sample increased and then decreased. Also, the sample which was sintered at 950 °C yielded the most intense emission spectra.

To accurately evaluate the luminescent properties of $ZnNb_2O_6$, the quantum efficiencies of selected samples sintered at 850 °C, 950 °C and 1050 °C were measured. As shown in Fig. S2 (see Supplementary information), the quantum efficiencies of the samples sintered at 850 °C, 950 °C and 1050 °C excited by 278 nm were 39%, 64% and 45%, respectively. Interestingly, the $ZnNb_2O_6$ sample sintered at 950 °C yielded the most intense emission spectra as well as the highest quantum efficiency up to 64%. We may expect that compound $ZnNb_2O_6$ could be used as a good solid state blue phosphor.

Conclusions

In this paper, we discovered that the crystal structure of a famous material, $ZnNb_2O_6$, was commensurately modulated for the first time. Through high-dimensional formalism, we established the structural model as (3+1)-D superspace group *Pbcn*(1/3 0 0)00*s*, which was comparable to previous reports of structural model of *Pbcn*. Powdered samples of $ZnNb_2O_6$ sintered at temperatures ranging from 800 ºC to 1150 ºC were prepared and the self-activated photoluminescent properties were characterized. The excitation wavelengths at about 276 nm, were associated with the charge transfer bands of the NbO_6 groups according to theoretical studies using the DFT method. The PL spectra under 278 nm excitation showed broad and strong blue emission peaks at about 470 nm. The sample sintered at 950 °C yielded the most intense emission spectra, which can achieve a high quantum efficiency up to 64%, thus we can say that compound $ZnNb_2O_6$ can be used as

a good blue phosphor. This work concerns the commensurately modulated structure of $ZnNb_2O_6$, and provides a deeper understanding of the crystal structure of the columbite-type compounds, which may help establish the relationship between the structure and properties for future researchers.

Acknowledgements

This work was supported by National Science Foundation of China with Grant (No. 11204067; 21307028).

References

1 H. J. Lee, K. S. Hong, S. J. Kim and I. T. Kim, *Mater. Res. Bull.*, 1997, **32**, 847-855.
2 M. Maeda, T. Yamamura and T. Ikeda, 1987, *Jpn. J. Appl. Phys. Suppl.*, **26**(2), 76-79.
3 A. Kudo, S. Nakagawa and H. Kato, *Chem. Let.*, 1999, 1197-1198.
4 Y. N. Sun, C. C. Gao, L. Tao, G. W. Wang, D. M. Han, C. Y. Li and H. H. Shan, *Catal. Commun.*, 2014, **50**, 73-77.
5 R. Wang, W. Zhang, Y. L. Xu and L. L. Xing, *Opt. &Laser Technol.*, 2014, **58**, 52-55.
6 K. Brandt and A. Kemi., *Mineral. Geol.*, 1943, **17A**, 1-8.
7 M. Waburg and H. K. Miiller-Buschbaum, *Z. Anorg. Allg Chem.*, 1984, **508**, 55-60.
8 A. I. Zaslavskii, Y. D. Kondrashev and S. S. Tolkachev, *Dokl. Akad. Nauk SSSR*, 1950, **75**, 559-561
9 T. Doert, B. P. T. Fokwa, P. Simon, S. Lidin and T. Sohnel, *Chem. -Eur. J.*, 2003, **9(23)**, 5865-5872.
10 A. Gagor, M. Weclawik, B. Bondzior and R. Jakubas, *CrystEngComm*, 2015, **17(17)**, 3286-3296.
11 R. F. Takagi, M. Johnsson and S. Lidin, *Chem. -Eur. J.*, 2008, **14(11)**, 3434-3441.
12 D. Zhao, R. H. Zhang, F. X. Ma and F. F. Li, *Mater. Lett.*, 2015, **157**, 219-221.
13 V. A. Morozov, A. Bertha, K. W. Meert, S. Van Rompaey, D. Batuk, G. T. Martinez, S. V. Aert, P. F. Smet, M. V. Raskina, D. Poelman, A. M. Abakumov and J. Hadermann, *Chem. Mater.*, 2013, **25(21)**, 4387-4395.
14 F. X. Wei, T. Baikie, T. An, M. Schreyer, C. Kloc and T. J. White, *J. Am. Chem. Soc.*, 2011, *133*, 15200–15211.
15 D. Dai, H. J. Koo and M. H. Whangbo, *Inorg. Chem.*, 2004, **43**, 4026-4035.
16 A. Arakcheeva, P. Pattison, A. Bauer-Brandl, H. Birkedal and G. Chapuis, *J. Appl. Crystallogr.*, 2013, **46(1)**, 99-107.
17 M. Zakhour-Nakhl, J. B. Claridge, J. Darriet, F. Weill, H.-C. zur Loye and J. M. Perez-Mato, *J. Am. Chem. Soc.*, 2000, **122(8)**, 1618-1623.
18 S. Sveleba, O. Semotyuk, I. Katerynchuk, Y. Furgala and Y. Pankivskyi, *Acta Phys. Pol. A*, 2006, **109(6)**, 695-700.
19 V. Hinkov, D. Haug, B. Fauqué, P. Bourges, Y. Sidis, A. Ivanov, C. Bernhard, C. Lin and B. Keimer, *Science*, 2008, **319(5863)**, 597-600.
20 V. Hinkov, S. Pailhes, P. Bourges, Y. Sidis, A. Ivanov, A. Kulakov, C. Lin, D. Chen, C. Bernhard and B. Keimer, *Nature*, 2004, **430(7000)**, 650-654.
21 Y. Gao, P. Lee, P. Coppens, M. Subramania and A. Sleight, *Science*, 1988, **241(4868)**, 954-956.
22 *Bruker. APEX2 and SAINT, Bruker AXS Inc.,* Madison, Wisconsin, USA, 2008.
23 L. Palatinus and G. Chapuis, *J. Appl. Crystallogr.*, 2007, **40**, 786-790.
24 V. Petricek, M. Dusek and L. Palatinus, *Z. Kristallogr.*, 2014, **229(5)**, 345-352.
25 M. Segall, P. Linda, M. Probert, C. Pickard, P. Hasnip, S. Clark and M. Payne, *Materials Studio CASTEP, Version 2.2*, San Diego, CA: Accelrys, Inc., 2002.
26 M. D. Segall, P. J. D. Lindan, M. J. Probert, C. J. Pickard, P. J. Hasnip, S. J. Clark and M. C. Payne, *J. Phys.: Condens. Matter.*, 2002, **14(11)**, 2717-2744.
27 J. Zhu, H. Chen, Y. D. Wang, S. Zhang, W. D. Cheng and H. T. Guan, *Chin. J. Struc. Chem.*, 2011, **30(5)**, 648-653.
28 D. R. Hamann, M. Schluter and C. Chiang, *Phys. Rev. Lett.*, 1979, **43**, 1494-1497.
29 I. D. Brown and D. Altermatt, *Acta Crystallogr., Sect. B: Struct. Sci.*, 1985, **41**, 244-247.
30 R. W. Godby, M. Schluther and L. J. Sham, *Phys. Rev. B*, 1987, **36**, 6497-6500.
31 C. M. I. Okoye, *J. Phys.: Condens. Matter*, 2003, **15**, 5945-5958.
32 M. Luo, G. Wang, C. Lin, N. Ye, Y. Zhou and W. Cheng, *Inorg. Chem.*, 2014, **53(15)**, 8098-8104.
33 Y. Y. Zhou, Z. F. Qiu, M. K. Lu, Q. Ma, A. Y. Zhang, G. J. Zhou, H. P. Zhang and Z. S. Yang, *J. Phys. Chem. C*, 2007, **111**, 10190-10193.
34 Y. J. Hsiao, T. H. Fang and L. W. Ji, *Mater. Lett.*, 2010, **64**, 2563–2565.

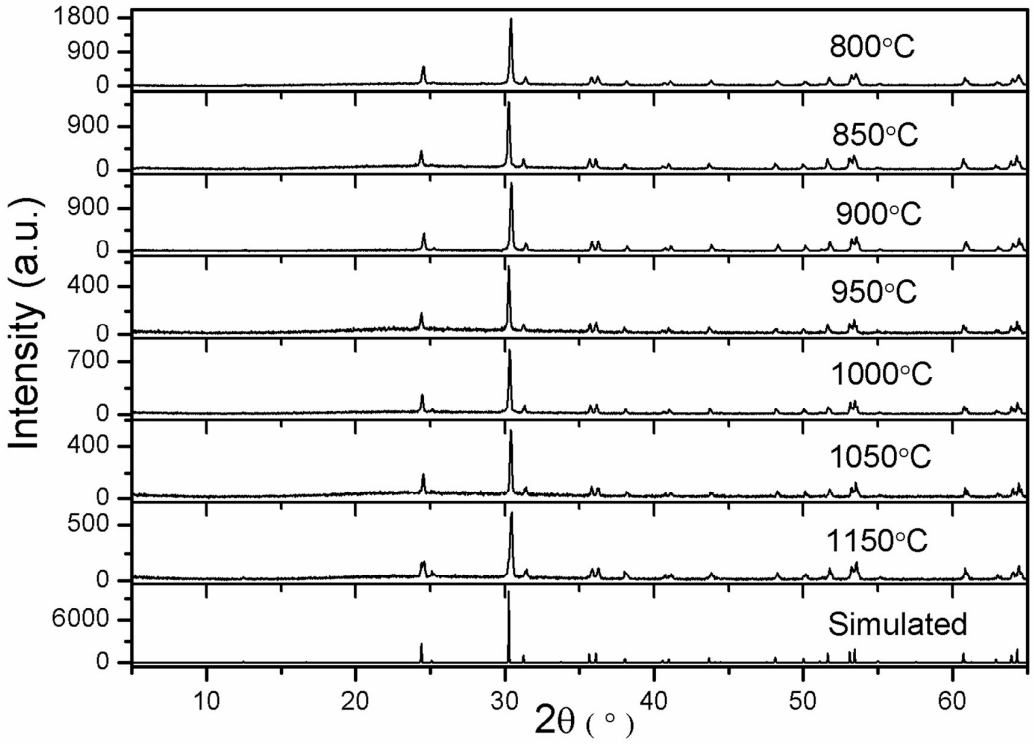

Figure 1. XRD pattern of $ZnNb_2O_6$ experimental sample compared with the simulated date from single-crystal date.

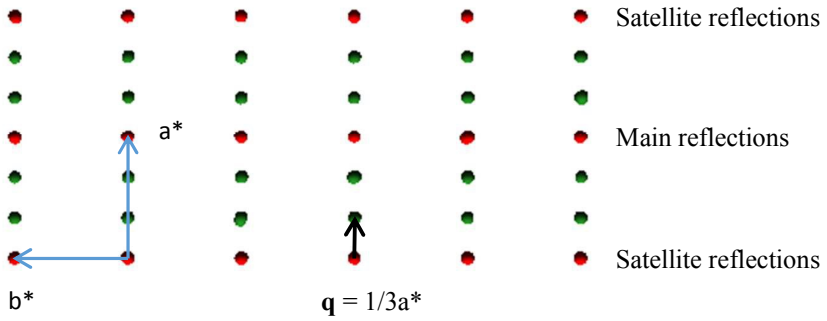

Figure 2. Reciprocal lattice view for $ZnNb_2O_6$ constructed from the experimental single crystal diffraction data showing the main reflections (red) and satellite reflections (green) down the and *c**-axis.

$NaMg(C_6H_6NO_6)\cdot H_2O$

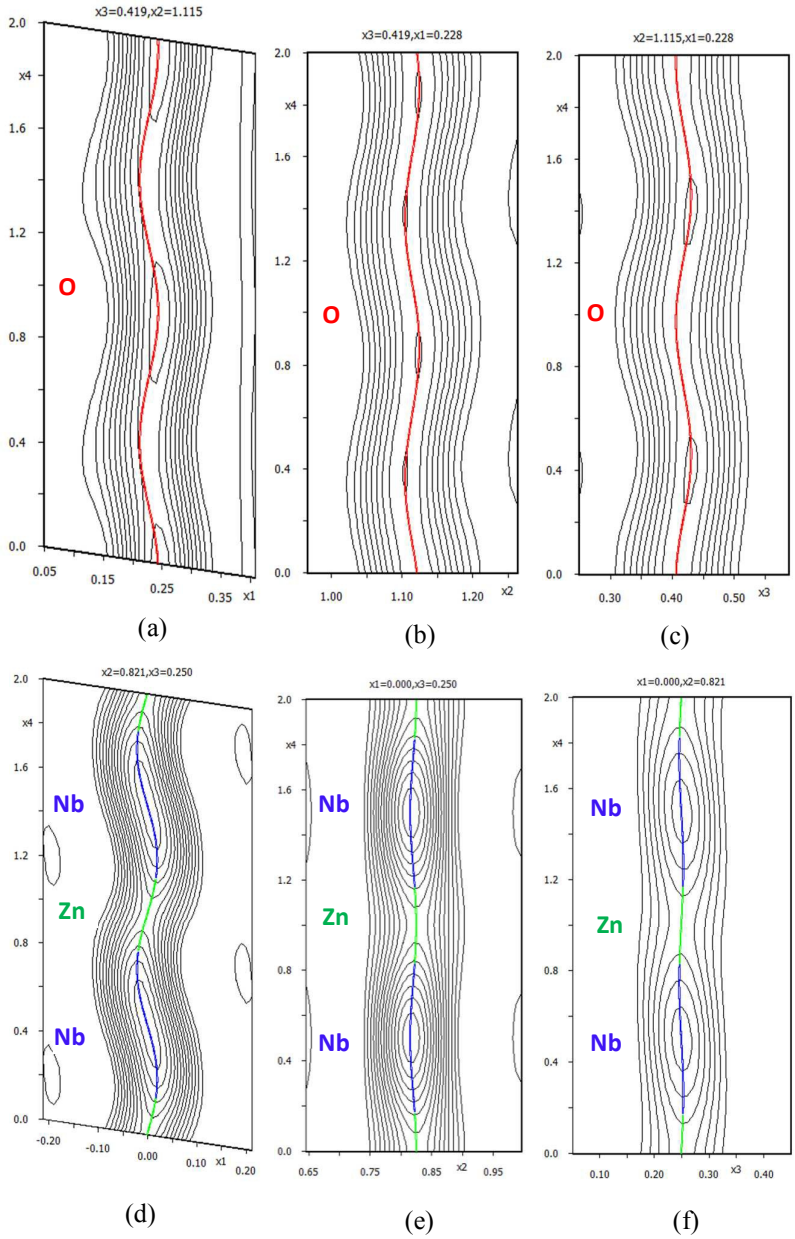

Figure 3. The vicinity of the O (a, b c) and $Zn_{0.333}|Nb_{0.667}$ (d, e, f) atom positions in the structural model. The x_1–x_4, x_2–x_4 and x_3–x_4 sections are presented, and the central lines correspond to calculated displacive modulation functions.

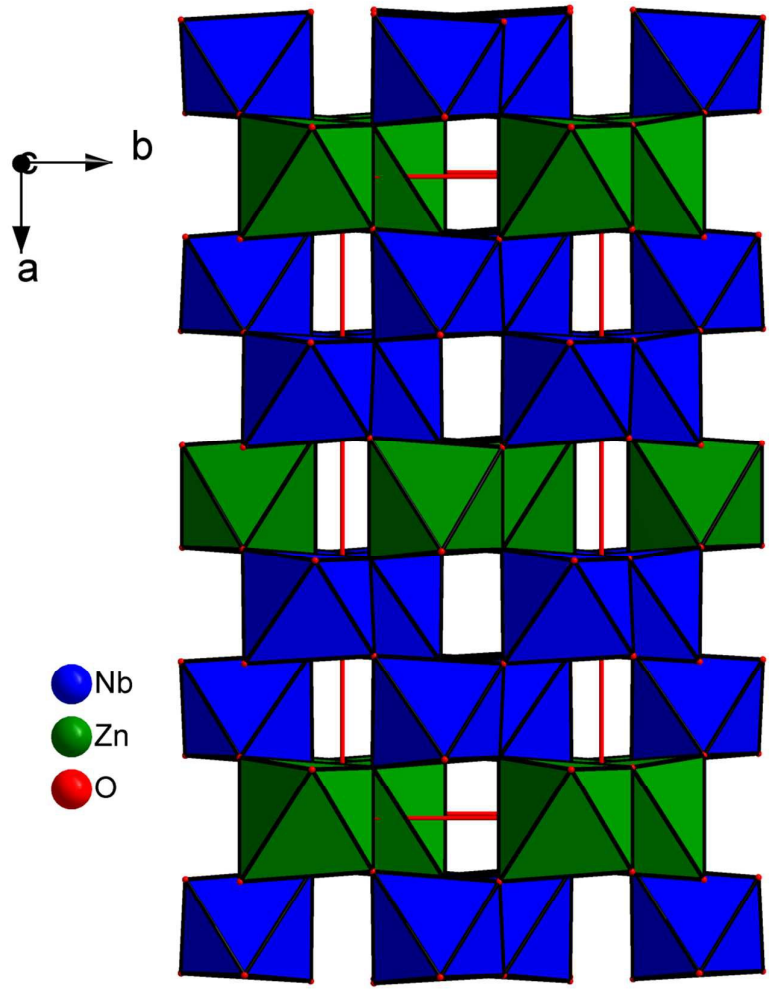

Figure 4. 3×*a* supercell of the commensurately modulated of $ZnNb_2O_6$ showing ZnO_6 and NbO_6 octahedra.

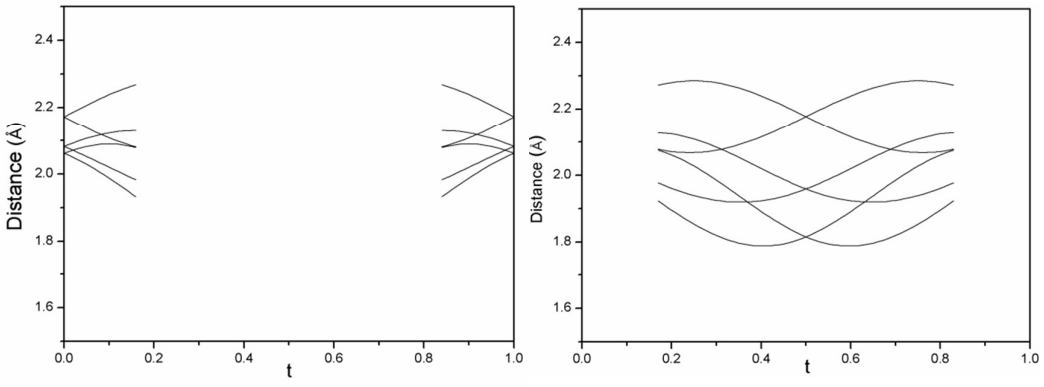

Figure 5. Evolution of Zn–O (a) and Nb–O (b) distances versus the internal parameter *t*.

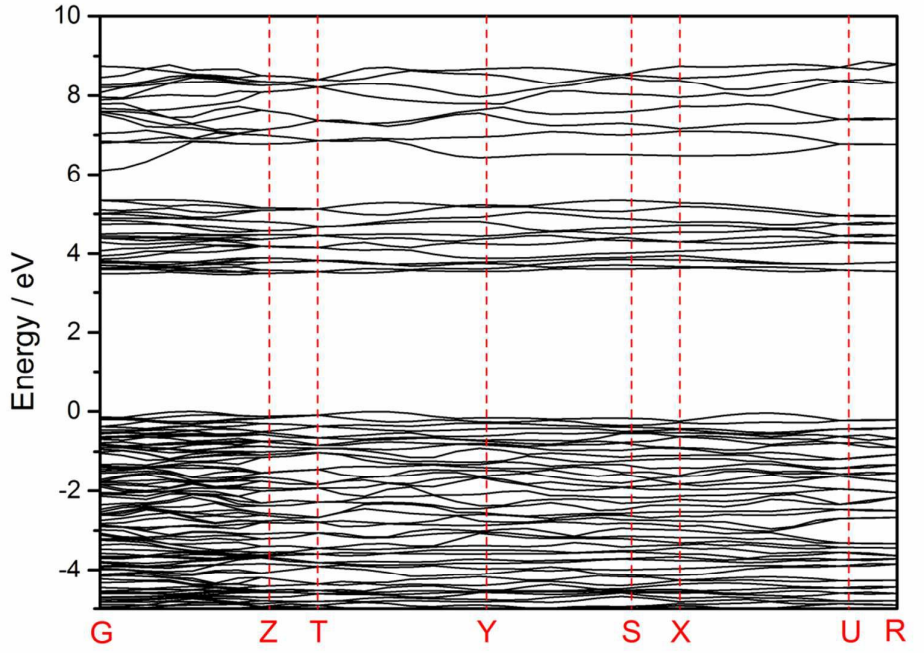

Figure 6. Calculated energy band structure of $ZnNb_2O_6$ in the range from -5.0 to 10.0 eV (the Fermi level is set at 0.0 eV).

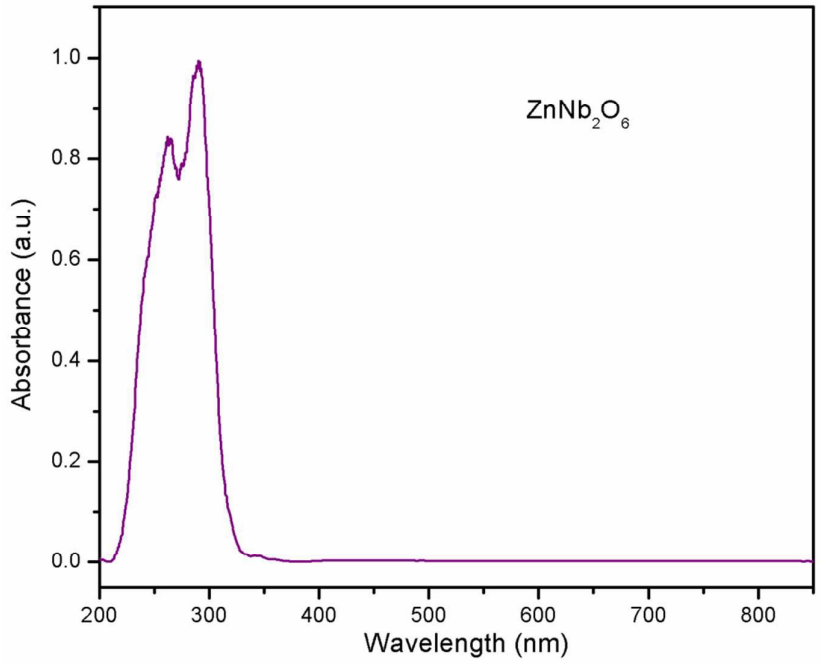

Figure 7. UV-Vis absorption spectra of $ZnNb_2O_6$ ranging from 200 to 850 nm.

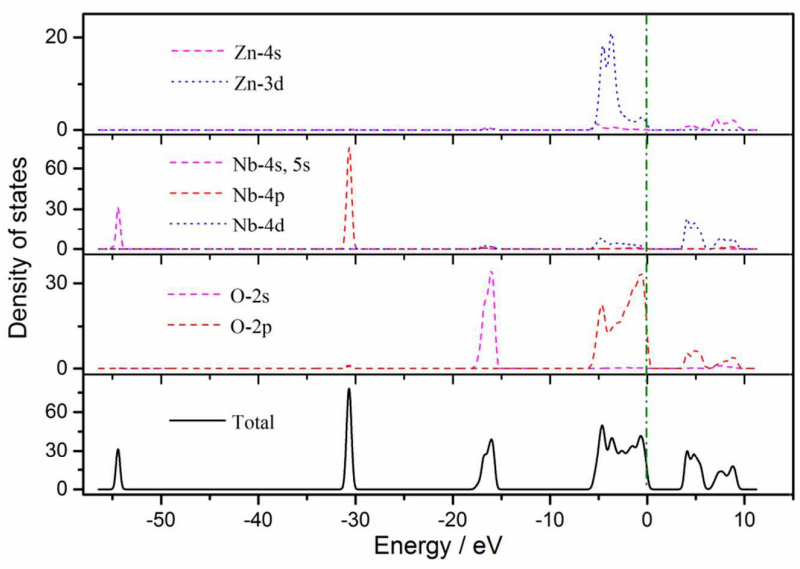

Figure 8. The total and partial DOS of $ZnNb_2O_6$

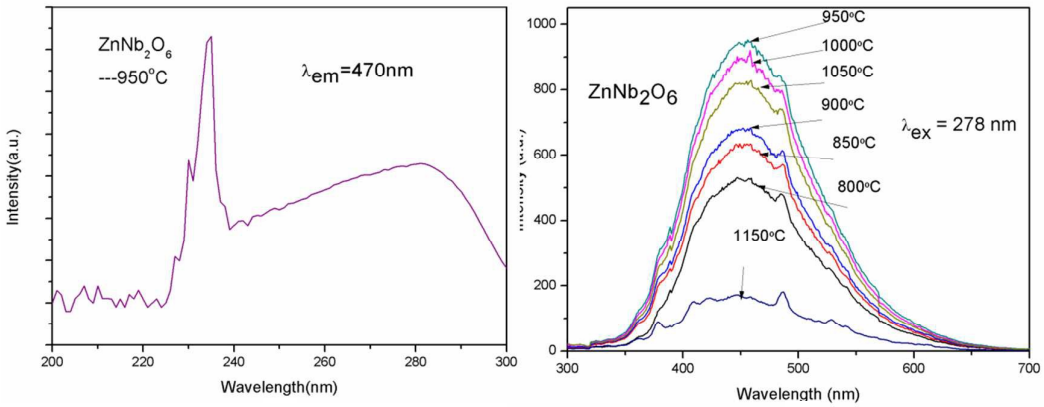

(a) (b)

Figure 9. Excitation spectra (a) and emission spectra (b) of $ZnNb_2O_6$

For the first time, this work reported the four-dimensional commensurately modulated structure of $ZnNb_2O_6$ using superspace formalism for aperiodic structures considering a modulation vector **q** = 1/3 *b**.

Positional and occupational modulations of commensurately modulated columbite-type compound $ZnNb_2O_6$